Real-Gas Scale Effects on Shuttle Orbiter Laminar Boundary-Layer Parameters

J.C. Adams Jr.,* W.R. Martindale,† A.W. Mayne Jr.,‡ and E.O. Marchand‡
ARO, Inc., Arnold Air Force Station, Tenn.

Inviscid and viscous (laminar boundary-layer) flowfield calculations under perfect-gas hypersonic wind tunnel and equilibrium real-gas flight conditions are presented for the windward centerline of the Space Shuttle Orbiter at a 30-deg angle of attack. Correlation parameters for laminar boundary-layer edge quantities and surface heat transfer are developed which properly account for entropy-layer-swallowing effects under both real-gas equilibrium and perfect-gas conditions.

Nomenclature

H = total enthalpy
h = static enthalpy
$\bar{h}$ = heat-transfer coefficient, $-\dot{q}_w/(T_{0,\infty}-T_w)$
$\bar{h}_{\text{ref}}$ = reference heat-transfer coefficient based on Fay-Riddell correlation and a scaled 1-ft spherical nose radius
L = reference length for 139 Orbiter, 1290.3 in. full scale
M = local Mach number
p_0' = freestream pitot pressure
p_p = local pitot pressure
p_w = wall static pressure
$\dot{q}_w$ = wall heat-transfer rate
r = radius as defined in Fig. 3
r_N = nose radius as defined in Fig. 3
Re = local unit Reynolds number
S = entropy-layer-swallowing similarity parameter, $(s/r_N)/Re_{\infty,rN}^{1/3}$
s' = surface distance from the sharp cone apex
s = surface distance from the stagnation point
St_e = local Stanton number based on local conditions at edge of boundary layer, $-\dot{q}_w/\rho_e U_e(H_\infty - h_w)$
T = temperature
U = velocity
u = tangential velocity in boundary layer
x', y' = freestream velocity-oriented coordinate system as defined in Fig. 2
x = axial distance in vehicle reference coordinate system as defined in Fig. 1
y = distance normal to the body surface
y_s = radius of shock for mass balance as defined in Fig. 3
α = vehicle angle of attack
δ = boundary-layer thickness
μ = viscosity
ρ = mass density

Subscripts

e = edge of boundary layer
conical = inviscid conical
H = based on total enthalpy
NS = based on isentropic expansion from stagnation point
0 = stagnation or total
t = onset of boundary-layer transition
w = wall
∞ = freestream

Received July 12, 1976; presented as Paper 76-358 at the AIAA 9th Fluid and Plasma Dynamics Conference, San Diego, Calif., July 14-16, 1976; revision received Dec. 16, 1976.

Index category: Boundary Layers and Convective Heat Transfer – Laminar.

*Supervisor, Project Support and Special Studies Section, Aerodynamics Projects Branch, von Karman Gas Dynamics Facility. Associate Fellow AIAA.

†Project Engineer, Aerothermodynamics Section, Aerodynamics Projects Branch, von Karman Gas Dynamics Facility.

‡Research Engineer, Project Support and Special Studies Section, Aerodynamics Projects Branch, von Karman Gas Dynamics Facility.

Introduction

HYPERSONIC wind tunnel data must be appropriately extrapolated to flight conditions by analytical methods if they are to be effectively utilized in vehicle design. In keeping with this, the primary objective of the present study is the development of correlation parameters which enable perfect-gas hypersonic wind tunnel data to be properly scaled to equilibrium real-gas flight conditions with respect to laminar boundary-layer edge quantities. The effects of entropy-layer swallowing, i.e., the entrainment of the flow which passed through the nose portion of the shock wave, must be considered if this objective is to be met. A secondary objective is the development of similarity parameters for correlation of surface heat transfer. The present study concerns the extrapolation to flight of the 30-deg angle-of-attack laminar boundary-layer edge condition and surface heat-transfer data obtained during the OH9[1] and OH4B[2] tests conducted in the AEDC von Karman Gas Dynamics Facility (VKF) Hypersonic Wind Tunnel (B) on the Space Shuttle Orbiter configuration. The approach used in the present work may be summarized as follows: 1) a realistic flowfield model, i.e., an equivalent axisymmetric body, amenable to existing AEDC/VKF analysis techniques was selected; 2) the laminar boundary-layer flow (including entropy-layer swallowing) was calculated for a range of perfect-gas wind tunnel and equilibrium real-gas flight conditions; and 3) the results were correlated in terms of aerodynamic parameters that can be effectively used in design studies.

Flowfield Model

Calculations from a flowfield model[3] developed for sharp-edged delta wings at incidence in hypersonic flow indicate that an angle-of-attack range exists where the windward centerline flowfield, both inviscid and viscous, is well approximated by a sharp cone at zero incidence having a half-angle equal to the angle of attack. In the case of an 80-deg-sweep delta wing at freestream Mach number 9.6, this angle-of-attack range extends from approximately 15 to 33 deg.[3] The windward surface of the Shuttle Orbiter (see Fig. 1) at values of x/L from 0.1 to 0.6 has a relatively flat bottom and a sweep angle of 80 deg. The windward centerline profile has a nearly continuous monotonically decreasing slope from the vehicle nose to an x/L value of 0.25. From this point the slope becomes constant at 1 deg (with respect to the vehicle reference system) up to an x/L value of 0.8.

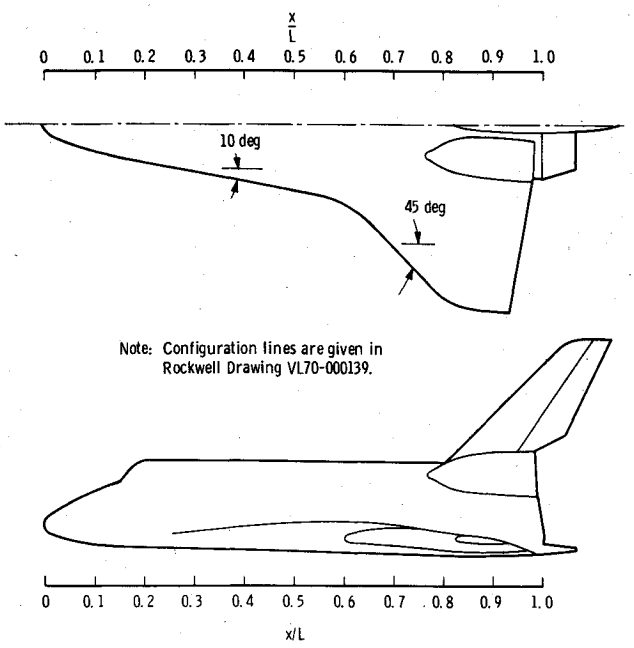

Fig. 1 Rockwell International 139 Space Shuttle Orbiter configuration.

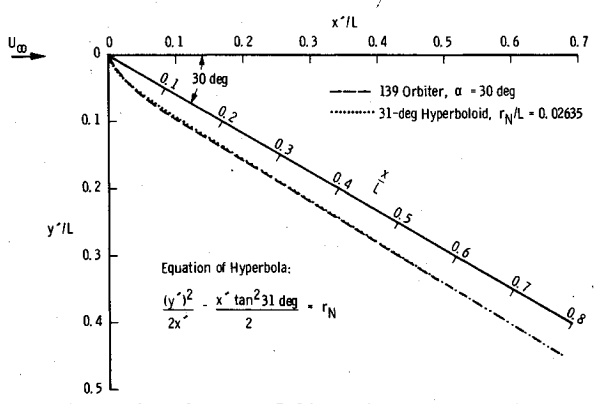

Fig. 2 Comparison between Orbiter windward centerline surface profile and a 31-deg asymptotic half-angle hyperboloid.

Based on the above discussion, a reasonable approximation of the windward centerline flowfield for the Shuttle Orbiter at 30 deg angle of attack should be an appropriate axisymmetric body at zero incidence. Use of a trial-and-error method with a model scale drawing showed that a 31-deg hyperboloid with a nose radius to body length value of 0.02635 has an excellent windward centerline profile comparison with the Shuttle Orbiter, as shown in Fig. 2.

Note that the coordinate system defined in Fig. 2 is aligned with the freestream velocity vector and that the origin is at the body point where the surface is normal to the freestream velocity. Also shown in Fig. 2 is the vehicle coordinate x/L. The correspondence of these coordinates and the surface distance coordinate s/r_N is given in Table 1.

Flowfield Calculation Methods

Boundary Layer and Inviscid Flow

The theory and numerical scheme used in obtaining the present boundary-layer results are based on the work of Patankar and Spalding.[4] The program, formulated by Mayne and Dyer,[5] embodies a number of significant modifications and extensions to the basic technique of Patankar and Spalding. These include elimination of the Couette flow analysis at the body surface and the so-called slip-value scheme in favor of applying the basic finite-difference scheme across the entire boundary layer.

Table 1 Coordinate correspondence[a]

x/L	x'/L	s/r_N
0.003	0	0
0.01	0.0061	0.74
0.02	0.0147	1.27
0.05	0.0407	2.59
0.10	0.0840	4.62
0.15	0.1273	6.59
0.20	0.1706	8.53
0.3	0.2572	12.40
0.4	0.3438	16.25
0.5	0.4304	20.11
0.6	0.5170	23.95
0.7	0.6036	27.79
0.8	0.6902	31.63

[a] $\alpha = 30$ deg.

Assuming the pressure along the outer edge of the boundary layer on a blunt body to have the inviscid surface value,§ the local edge flow conditions are determined by consideration of the inclination of the bow shock where the local flow streamline crossed the shock. The point at which the flow along the edge of the boundary layer crossed the shock can be determined by matching the mass flow in the boundary layer at a given location to the freestream mass flow in a cylinder with radius extending out to the location to be determined. Referring to Fig. 3, this may be expressed as

$$\rho_\infty U_\infty \pi y_s^2 = \int_0^{y_e} 2\pi r \rho u dy \qquad (1)$$

Note that y_e is the thickness of the region over which the boundary-layer equations are being solved. After y_s is found, the shock inclination at that point can be determined and the flow conditions along the boundary layer at the corresponding body location can be computed by crossing the oblique shock at y_s with the freestream flow and allowing that flow to expand isentropically to the known local boundary-layer edge pressure. Naturally, an entropy-layer-swallowing analysis such as described above requires that the shape of the bow shock be known in addition to the body surface pressure. In the present calculations, these data for both real- and perfect-gas conditions were obtained from a method-of-characteristics solution using the digital computer code developed by Inouye, Rakich, and Lomax.[6] For the perfect-gas cases, the finite-difference method of Aungier[7] was used to determine the blunt nose subsonic region solutions for input to the downstream perfect-gas method-of-characteristics analysis. For the real-gas (equilibrium air) cases, the inverse method of Lomax and Inouye[8] was used to determine the blunt nose subsonic region solutions for input to the downstream real-gas method-of-characteristics analysis.

§This assumption should be valid as long as the pressure gradient normal to the body surface is small. This is also consistent with the formulation of the boundary-layer equations.

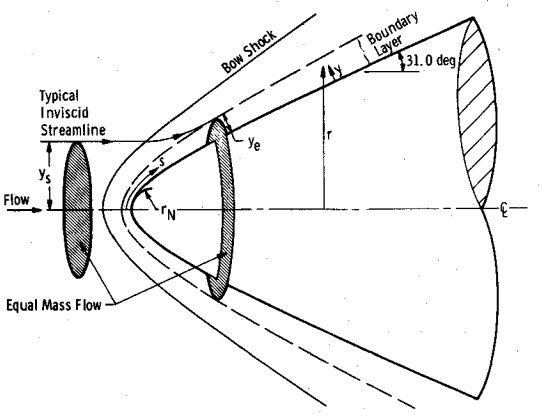

Fig. 3 Hyperboloid geometry, showing inviscid streamline swallowing.

When entropy swallowing is being considered, the definition of the outer edge of the boundary layer must be reconsidered. This is necessary because the velocity and temperature gradients are not zero at the outer edge of the boundary layer but have values associated with the inviscid flowfield. This is the result of the combination of the entropy-layer swallowing and the use of the nonsimilar boundary-layer equations. To treat this situation, one may define the boundary-layer thickness in terms of the total enthalpy, since the gradient of this quantity does go to zero at the boundary-layer edge. This approach, proposed by Levine,[9] was used herein. In particular, the region treated by the boundary-layer equations was adjusted so that y_e was a minimum of 1.1 times the value of y where

$$(H-h_w)/(H_\infty-h_w)=0.999 \qquad (2)$$

Consideration of the total enthalpy profile behavior also allows a boundary-layer thickness to be defined in terms of the deviation of H/H_∞ from unity. A total enthalpy boundary-layer thickness, δ_H, has been defined as the distance from the body surface to the point where H/H_∞ differs from unity by 0.005, when approached from the outer part of the flow. For hot-wall cases with overshoot in H/H_∞ (i.e., values greater than one), this means that δ_H is at $H/H_\infty=1.005$ where $dH/dy\leq 0$. For cases with no overshoot, it merely means that δ_H is at $H/H_\infty=0.995$.

Calculations for the real-gas flight conditions in the present study treat the flow as dissociating air in thermodynamic equilibrium using the thermodynamic and transport property correlation formulas of Cohen.[10] Under hypersonic wind tunnel conditions, the flow is taken to be thermally and calorically perfect air with a constant Prandtl number of 0.7 in conjunction with Sutherland's viscosity law.

A more complete discussion of entropy-layer swallowing by laminar boundary layers, including comparisons of results from boundary-layer analyses which include and exclude entropy-swallowing effects relative to a fully viscous shock-layer method, is given by Mayne and Adams.[11]

Freestream Conditions

Wind Tunnel

Table 2 gives a set of three freestream conditions in Tunnel B for which data were taken during recent tests.[1,2,12] The first condition corresponds to the OH9 test[1,12] where the boundary-layer edge conditions were measured via flowfield probe surveys. Model wall temperatures were also measured at this test condition; these values are tabulated in Table 2. The other two freestream conditons in Table 2 correspond to the maximum and minimum Reynolds number conditions of the OH4B heat-transfer test.[2] It should be noted that these are the maximum and minimum Reynolds numbers available in Tunnel B. Model wall temperatures for these conditions are also tabulated in Table 2.

Note the case designation 1T, 2T, and 3T in Table 2. This designation will be used in the remainder of this paper to identify the wind tunnel conditions.

Flight

Table 3 gives the set of ten altitude-velocity flight conditions considered. The corresponding freestream properties were taken from altitude-velocity tables,[13] which are based on the 1962 U.S. Standard Atmosphere. The numerical case designation numbers will be used in the remainder of this paper to identify the flight conditions.

Radiative equilibrium wall temperature distributions were input to the boundary-layer calculations to properly take into account variable wall temperature effects on the entropy-layer-swallowing phenomenon under flight conditions. These temperatures varied from 2600 to 1100°F depending on trajectory point and distance from the vehicle nose.

Flowfield Model Verfication under Hypersonic Wind Tunnel Conditions

In order to verify the applicability of the axisymmetric flowfield model postulated above, comparisons have been made between the present analysis techniques and experimental measurements. Figure 4 presents the measured windward centerline and calculated inviscid flowfield properties. The surface pressure distribution shown in Fig. 4 reveals relatively good agreement between measured and calculated values. The same is true of the shock shape comparison shown in Fig. 4. Note that the differences between measured and calculated shock shape coordinates are consistent with the differences in body shape coordinates shown previously relative to Fig. 2.

A comparison between measured and calculated local boundary-layer edge parameters is given in Fig. 5. The

Table 2 Tunnel B conditions[a]

Case	M_∞	Re_∞/ft	Re_{∞,r_N}	$T_{0,\infty}$, °R	$T_w/T_{0,\infty}$
1T	7.92	681,614	33,794	1332	0.86→0.45 5
2T	8.00	3,706,270	183,757	1351	0.42
3T	7.92	541,605	26,853	1263	0.43

[a] Re_{∞,r_N} is based on a nose radius of 0.04958 ft.

Table 3 Reference trajectory[a]

Case	Time, sec	Altitude, ft	Velocity, ft/sec	M_∞	Re_∞/ft	Re_{∞,r_N}
1	400	269,915	26,006	29.41	2,610	7,395
2	496	252,149	25,576	28.01	6,064	17,181
3	608	243,742	24,727	26.38	8,193	23,213
4	704	239,322	23,864	25.14	9,390	26,605
5	800	233,529	22,897	23,73	11,214	31,773
6	896	225,698	21,767	22.09	14,177	40,168
7	1008	212,699	20,119	19.74	20,525	58,154
8	1104	195,803	18,148	17.22	32,755	92,806
9	1200	186,076	15,665	14.70	39,921	113,109
10	1296	178,440	13,310	12.39	44,194	125,216

[a] Re_{∞,r_N} is based on a nose radius of 2.83333 ft. For this trajectory 29.5 deg $\leq\alpha\leq$ 31.6 deg; all calculations assume $\alpha=30$ deg.

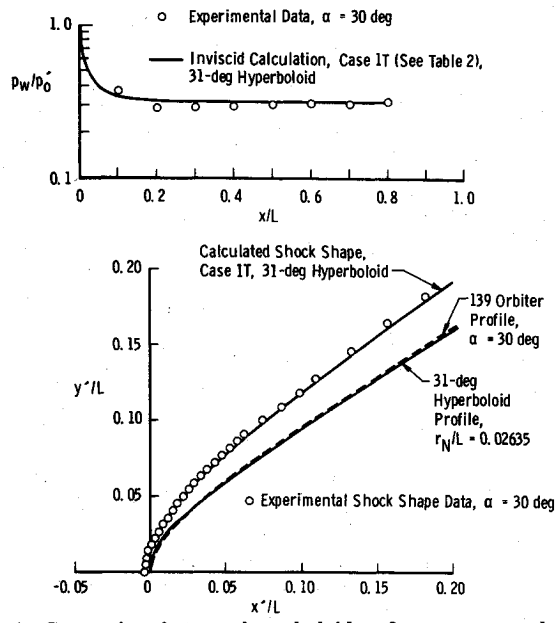

Fig. 4 Comparison between hyperboloid surface pressure and shock shape calculations and AEDC/VKF Tunnel B data.

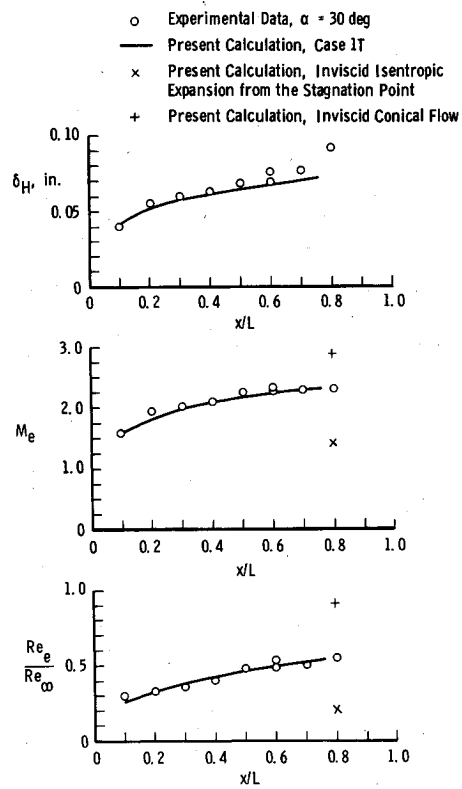

Fig. 5 Comparison between hyperboloid boundary-layer edge parameter calculations and data.

boundary-layer edge conditons are based on a total enthalpy definition of the boundary-layer thickness, δ_H. Each of the parameters shown in Fig. 5 reveals good agreement between experiment and calculations. It is important to observe the entropy-layer-swallowing phenomenon as typified by the edge Mach number and edge Reynolds number distributions relative to the corresponding limiting values for inviscid conical flow and inviscid normal shock-isentropic expansion. Entropy-layer swallowing is of importance over the entire body for this particular configuration and laminar flow condition.

Calculated and measured windward centerline boundary-layer profiles are compared in Fig. 6 for the body location

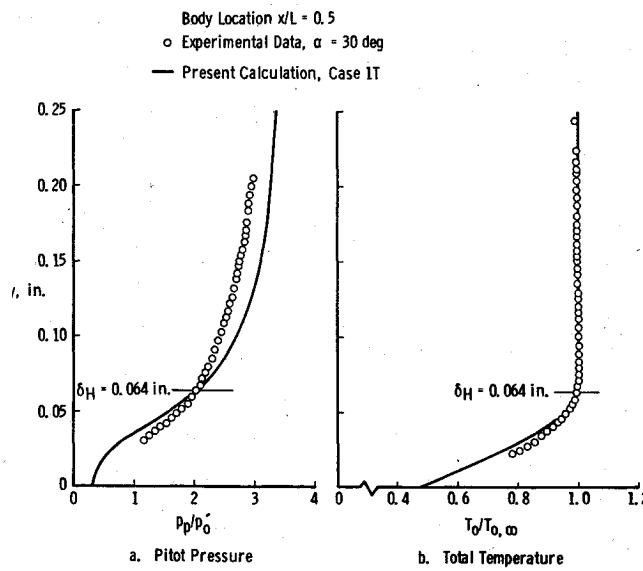

Fig. 6 Comparison between hyperboloid boundary-layer profile calculations and data.

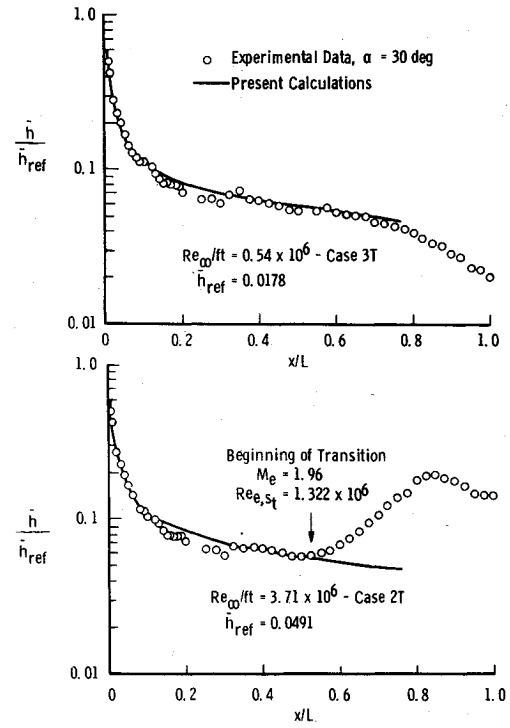

Fig. 7 Comparison between hyperboloid surface heat-transfer calculations and data.

$x/L = 0.5$. Indicated on each figure is the calculated boundary-layer thickness, δ_H, based on the total enthalpy definition. As can be seen from Fig. 6a, pitot pressure measurements alone cannot be used to experimentally define the viscous-inviscid interface (i.e., the boundary-layer thickness) under hypersonic flow conditions where entropy-layer swallowing is important. Total temperature measurements, such as are shown in Fig. 6b, are required for such flows. It should be noted that the experimental measurements shown in Fig. 6a and b have been corrected for pressure lag error and radiation losses.[12]

The measured (via the thin-skin thermocouple technique) and calculated surface heat-transfer distribuions as reflected through $\bar{h}/\bar{h}_{ref}$ are given in Fig. 7. The comparison is quite good except in the region of $0.15 < x/L < 0.30$ where the measured heat-transfer rates are slightly lower than the

calculated values. This is consistent with the surface pressure distribution shown previously in Fig. 4.

Note that in the lower portion of Fig. 7 the boundary-layer edge Mach number and edge Reynolds number at the onset of boundary-layer transition are indicated based upon the present entropy-layer-swallowing laminar boundary-layer calculations. In the absence of experimental flowfield data at a particular test conditon, an entropy-layer swallowing boundary-layer calculation is the only way in which these values can be obtained.

The results shown in Figs. 4-7 clearly indicate that application of the axisymmetric flowfield model and the entropy-layer-swallowing boundary-layer calculation methods results in realistic values of measurable flowfield and surface parameters for the Orbiter at 30 deg angle of attack under hypersonic wind tunnel conditions. It is therefore reasonable to assume that, by using equilibrium air properties in the present calculation methods, realistic flowfield calculations can be obtained under real-gas flight conditons, if the flow is indeed close to equilibrium.

Correlation of Boundary-Layer Parameters Including Effects of Entropy-Layer Swallowing

Following Rotta and Zakkay,[14] whose work is based on earlier work by Ferri,[15] Zakkay and Krause,[16] and Rubin,[17] there is sound theoretical justification for choosing the following form of a similarity parameter (denoted hereafter as S) for the entropy-layer-swallowing process.

$$S = \frac{s/r_N}{Re_{\infty,r_N}^{1/3}} \tag{3}$$

The similarity parameter, S, is not applicable in the nose region of the body; neither is it applicable for very low Reynolds number flows. It is assumed that the range of current interest, namely $0.10 \leq S \leq 1.0$, is a reasonable choice for the present flow conditions. All succeeding figures which employ the similarity parameter, S, will be restricted to this range.

Examination of the calculated results for flight cases 1 through 10 and wind tunnel cases 1T through 3T has revealed the following correlation parameters for the outer edge boundary-layer parameters:

Outer edge quantity	Correlation parameter
M_e	$\frac{M_e/M_{e,NS}}{M_{\text{conical}}}$
Re_e	$\frac{Re_e/Re_{e,NS}}{M_\infty^{0.70}}$

Logarithmic plots which show a data band encompassing flight cases 1 through 10 and wind tunnel cases 1T through 3T and a mean fit to the data band are presented in Figs. 8 and 9 for the outer edge Mach number and outer edge Reynolds number correlation parameters, respectively. Also indicated by closed circles on the figures are the experimental data from the Tunnel B flowfield survey. It is important to observe from Figs. 8 and 9 that the maximum deviation from the mean fit to the data band is only approximately $\pm 10\%$.

Under hypersonic flow conditions where entropy-layer-swallowing effects are important, classical laminar boundary-layer parameters such as displacement thickness and momentum thickness become ill-defined due to gradients in the boundary-layer velocity and static density profiles at the outer edge of the boundary layer. A boundary-layer parameter which has physical meaning under these conditions is a boundary-layer thickness based upon the total enthalpy definition of the boundary-layer edge. Classical laminar boundary-layer theory for a sharp cone at zero angle of attack

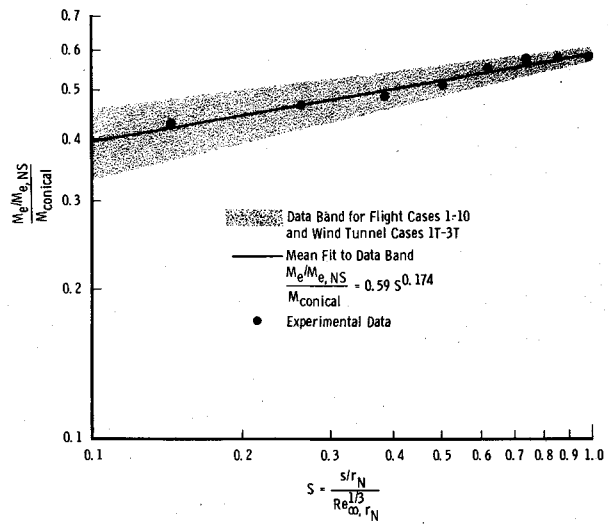

Fig. 8 Logarithmic plot of the laminar boundary-layer outer edge Mach number correlation parameter.

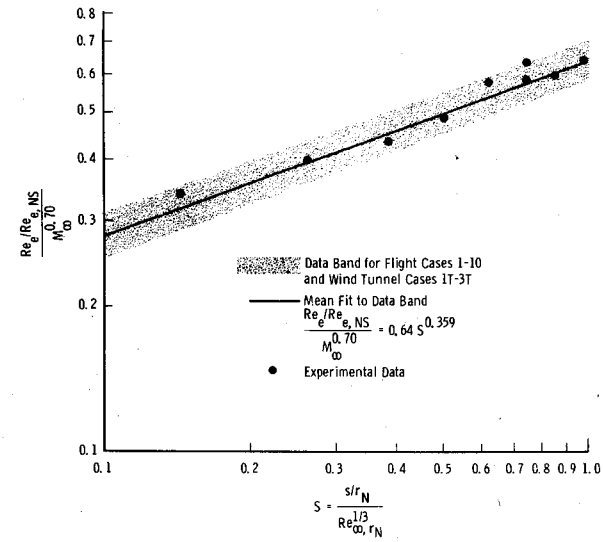

Fig. 9 Logarithmic plot of the laminar boundary-layer outer edge unit Reynolds number correlation parameter.

in a supersonic or hypersonic flow indicates that the boundary-layer thickness, δ, is given by an expression of the form

$$(\delta/s')\,(Re_{e,s'})^{1/2} = f(M_\infty, \text{etc.}) \tag{4}$$

In an analogous manner, it is reasonable to postulate that the laminar boundary-layer thickness, δ_H, based on a total enthalpy definition under conditions where entropy-layer swallowing is important can be correlated by an expression of the form

$$(\delta_H/s)\,(Re_{e,s})^{1/2} = f(M_\infty, \text{etc}) \tag{5}$$

which can be written as

$$\frac{(\delta_H/r_N)\,(Re_{e,r_N})^{1/2}}{Re_{\infty,r_N}^{1/6}} = f(M_\infty, \text{etc.})\left(\frac{s/r_N}{Re_{\infty,r_N}^{1/3}}\right)^{1/2}$$

$$= f(M_\infty, \text{etc.})(S)^{1/2} \tag{6}$$

A logarithmic plot of this correlation parameter for total enthalpy-defined boundary-layer thickness is given in Fig. 10 as a function of all ten real-gas flight conditions and the three perfect-gas wind tunnel conditions. A weak freestream Mach

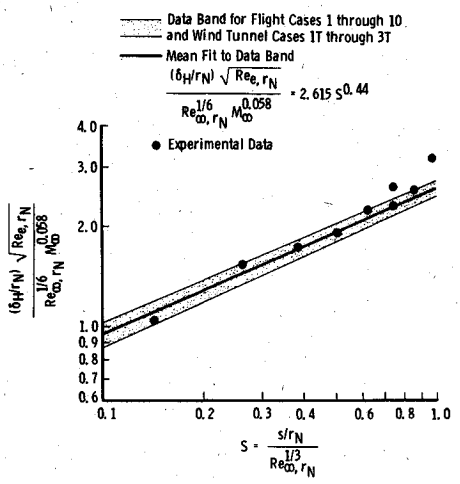

Fig. 10 Logarithmic plot of the laminar boundary-layer thickness correlation parameter.

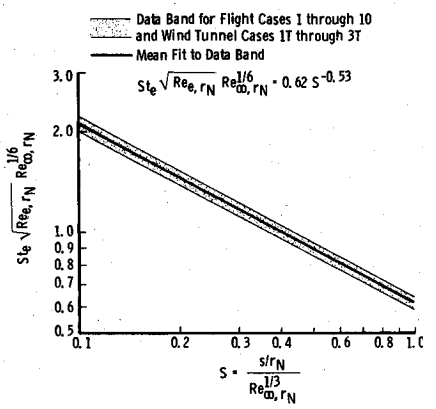

Fig. 11 Logarithmic plot of the laminar boundary-layer surface heat-transfer correlation parameter.

number influence on the correlation parameter is shown in Fig. 10, namely

$$\frac{(\delta_H/r_N)\,(Re_{e,r_N})^{1/2}}{Re_{\infty,r_N}^{1/6} M_\infty^{0.058}} \tag{7}$$

which is based upon examination of the freestream Mach number effect at a common value of the similarity parameter, S. Examination of Fig. 10 reveals that the correlation parameter for total enthalpy-defined boundary-layer thickness yields correlated results within $\pm 10\%$ maximum deviation from the mean fit to the data band. Note also the experimental data (indicated by closed circles) from the Tunnel B flowfield survey.

Classical laminar boundary-layer theory for a sharp cone at zero angle of attack in a supersonic or hypersonic flow indicates that the surface heat transfer is given by an expression of the form

$$St_e\,(Re_{e,s})^{1/2} = f(M_\infty, \text{etc.}) \tag{8}$$

In an analogous manner, it is reasonable to postulate that the laminar boundary-layer surface heat transfer under conditions where entropy-layer swallowing is important can be correlated by an expression of the form

$$St_e\,(Re_{e,s})^{1/2} = f(M_\infty, \text{etc.}) \tag{9}$$

which can be written as

$$St_e\,(Re_{e,r_N})^{1/2} Re_{\infty,r_N}^{1/6} = f(M_\infty, \text{etc.}) \Big/ \left(\frac{s/r_N}{Re_{\infty,r_N}^{1/3}}\right)^{1/2} = f(M_\infty, \text{etc.})/S^{1/2} \tag{10}$$

A logarithmic plot of the above proposed correlation parameter for surface heat transfer is given in Fig. 11. It is to be noted that no freestream Mach number effect could be discerned from examination of the data. As can be seen from Fig. 11, the above proposed correlation parameter for surface heat transfer yields correlated results within $\pm 10\%$ maximum deviation from the mean fit to the data band. The key points in this successful application are the determination of the local mass flux and the use of the local wall enthalpy in the Stanton number expression.

Concluding Summary

The present investigation has resulted in development of correlation parameters for laminar boundary-layer edge quantities and surface heat transfer along the windward symmetry plane of the Space Shuttle Orbiter configuration at 30 deg angle of attack. These correlation parameters enable hypersonic wind tunnel data to be properly scaled to flight under conditions where entropy-layer swallowing by the boundary layer must be considered. The proposed correlation parameters are simple to use (in an engineering sense) and accurately account for real-gas (equilibrium air) effects as encountered in flight.

Acknowledgment

The research reported herein was conducted by the Arnold Engineering Development Center (AEDC), Air Force Systems Command (AFSC), U.S. Air Force, for the Rockwell International Space Division under sponsorship of the National Aeronautics and Space Administration (NASA/JSC). Research results were obtained by personnel of ARO, Inc., contract operator of AEDC.

References

[1]Quan, M., "Results of Tests on a Rockwell International Space Shuttle Orbiter (139 Configuration) 0.0175-Scale Model (No. 29-0) in AEDC Tunnel B to Determine Boundary Layer Characteristics (OH9)," NASA-CR-141,540, May 1975.

[2]Foster, T.F. and Grifall, W.J., "Data Report for Tests on the Heat Transfer Effects of the 0.0175-Scale Rockwell International Space Shuttle Vehicle Model 22-OT in the AEDC 50-in B Wind Tunnel, Vols. I, II, III," NASA-CR-134, 419, NASA-CR-134, 438, NASA-CR-134, 439, Feb. 1975.

[3]Nagel, A.L., Fitzsimmons, H.D., and Doyle, L.B., "Analysis of Hypersonic Pressure and Heat Transfer Tests on Delta Wings with Laminar and Turbulent Boundary Layers," NASA CR-535, Aug. 1966.

[4]Patankar, S.V. and Spalding, D.B., *Heat and Mass Transfer in Boundary Layers*, CRC Press, Cleveland, Ohio, 1968.

[5]Mayne, A.W. Jr. and Dyer, D.F., "Comparisons of Theory and Experiment for Turbulent Boundary Layers on Simple Shapes at Hypersonic Conditions," *Proceedings of the 1970 Heat Transfer and Fluid Mechanics Institute*, Stanford University Press, June 1970, pp. 168-188.

[6]Inouye, M., Rakich, J.V., and Lomax, H., "A Description of Numerical Methods and Computer Programs for Two-Dimensional and Axisymmetric Supersonic Flow over Blunt-Nosed and Flared Bodies," NASA TN D-2970, Aug. 1965.

[7]Aungier, R.H., "A Computational Method for Exact, Direct, and Unified Solutions for Axisymmetric Flow Over Blunt Bodies of Arbitrary Shape (Program BLUNT)," AFWL-TR-70-16, July 1970.

[8]Lomax, H. and Inouye, M., "Numerical Analysis of Flow Properties About Blunt Bodies Moving at Supersonic Speeds in an Equilibrium Gas," NASA TR R-204, July 1964.

[9]Levine, J.N., "Finite Difference Solution of the Laminar Boundary-Layer Equations Including Second-Order Effects," AIAA Paper 68-739, presented at the AIAA Fluid and Plasma Dynamics Conference, Los Angeles, Calif., 1968.

[10]Cohen, N.B., "Correlation Formulas and Tables of Density and Some Transport Properties of Equilibrium Dissociating Air for Use in Solutions of the Boundary-Layer Equations," NASA TN D-194, Feb. 1960.

[11]Mayne, A.W. Jr. and Adams, J.C. Jr., "Streamline Swallowing by Laminar Boundary Layers in Hypersonic Flow," AEDC-TR-71-32 (AD719748), March 1971.

[12]Martindale, W.R. and Carter, L.D., "Flowfield Measurements in the Windward Surface Shock Layer of Space Shuttle Orbiter Configurations at Mach Number 8," AEDC-TR-75-5 (AD-A012875), July 1975.

[13]Lewis, C.H. and Burgess, E.G. III, "Altitude-Velocity Table and Charts for Imperfect Air," AEDC-TDR-64-214 (AD454078), Jan. 1965.

[14]Rotta, N.R. and Zakkay, V., "Effects of Nose Bluntness on the Boundary Layer Characteristics of Conical Bodies at Hypersonic Speeds," *Astronautica Acta*, Vol. 13, Aug. 1968, pp. 507-516.

[15]Ferri, A., "Some Heat Transfer Problems in Hypersonic Flow," *Aeronautics and Astronautics*, Pergamon Press, New York, 1960, pp. 344-377.

[16]Zakkay, V. and Krause, E., "Boundary Conditions at the Outer Edge of the Boundary Layer on Blunted Conical Bodies," *AIAA Journal*, Vol. 1, July 1963, pp. 1671-1672.

[17]Rubin, I., "Shock Curvature Effect on the Outer Edge Conditions of a Laminar Boundary Layer," *AIAA Journal*, Vol. 1, Dec. 1963, pp. 2850-2852.